Eur. Phys. J. D **41**, 349–354 (2007)
DOI: 10.1140/epjd/e2006-00238-4

THE EUROPEAN PHYSICAL JOURNAL D

Combination of two basic types of synchronization in a coupled semiconductor laser system

L. Wu[1,a], S. Zhu[1,b], and Y. Ni[2]

[1] School of Physical Science and Technology, Suzhou University, Suzhou, Jiangsu 215006, P.R. China
[2] Basic Course Department, Suzhou Polytechnical Institute of Agriculture, Suzhou, Jiangsu 215004, P.R. China

Received 13 March 2006 / Received in final form 6 September 2006
Published online 1st November 2006 –

Abstract. Combination of two basic types of synchronization, anticipatory synchronization and lagged synchronization, is investigated numerically between two coupled semiconductor lasers. It is found that lagged synchronization produced by a backward coupling with a suitable delay can combine with the originally hidden anticipatory synchronization and produce a type of synchronization overcoming the original lagged synchronization produced by a forward coupling. We study the combination synchronization phenomenon when the delay of the backward coupling is different from that of the original anticipatory synchronization. Our results suggest that the synchronization combination phenomenon might allow an interpretation of an experimental observation by Sivaprakasam et al. [Phys. Rev. Lett. **87**, 154101 (2001)] that the anticipating time is irrespective of the external-cavity round trip time, which to date remains to be understood.

PACS. 05.45.Xt Synchronization; coupled oscillators – 42.55.Px Semiconductor lasers; laser diodes – 42.65.Sf Dynamics of nonlinear optical systems; optical instabilities, optical chaos and complexity, and optical spatio-temporal dynamics

1 Introduction

During the last few decades, much attention has been paid to chaotic synchronization because of its potential applications in a wide variety of fields, especially in communication [1–6]. Recent works have focused upon coupled semiconductor lasers operating in the Low-Frequency-Fluctuation (LFF) regime [7–12], where the intensity output of the laser exhibits irregular dropout events (sisyphus effect, see [13]). Sudden reduction in output due to a dropout is followed by a gradual recovery until another dropout occurs [13–17]. The interval between dropouts is irregular [18–21] and two lasers without interaction should experience several irregular and uncorrelated dropouts. However the coupling of two lasers by injecting part of the output of one laser (laser 1) into the other (laser 2) may produce correlated outputs, particularly regarding dropouts [22]. In other words, the dropouts of laser 1 are transferred into the output of laser 2, due to which the dropouts of the two lasers occur in the same rate, thus achieving a synchronization of the involved lasers. Such synchronization does not always achieve exact equality of the outputs of the two lasers, but it can be considered as a chaos control mechanism for the LFF behavior of laser 2 by laser 1. In specific circumstances even a complete synchronization can be obtained [23–25].

[a] e-mail: liangwu@suda.edu.cn
[b] e-mail: szhu@suda.edu.cn, corresponding author

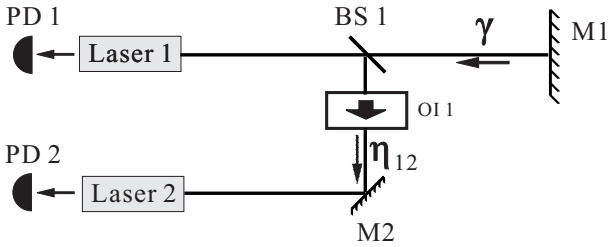

Fig. 1. Schematic representation of the unidirectional coupled laser system, where two basic types of synchronization are typically shown.

The unidirectional coupled laser system is shown in Figure 1. A part of the output of laser 1 is fed back by a mirror M1. Another part is injected into laser 2 via a beam splitter BS1, an optical isolator OI1 (to ensure there is no light from laser 2 to enter laser 1 and alter the dynamics of laser 1) as well as another mirror M2. No feedback is used within laser 2. Photo diodes (PD1, 2) are used to detect the outputs of the two lasers respectively. The feedback rate is labeled by γ. The coupling strength from laser 1 to laser 2 is represented by η_{12}.

Through a simple analysis of the rate equations for the unidirectional coupled laser system, two types of synchronization have been identified when the coupling retardation time for light to travel from laser 1 to laser 2 is τ_{c12}

and the external cavity round trip time in laser 1 is τ [26–32]

Anticipatory Synchronization (AS):

$$I_2(t-\tau) \sim I_1(t-\tau_{c12}), \quad (1)$$

Lagged Synchronization (LS): $I_2(t) \sim I_1(t-\tau_{c12})$. (2)

The system is able to choose one type of synchronization, while the other is hidden. The choice is determined by the competition between the two types. A transition from one type to the other may occur if operating parameters are changed [29,33,34]. But in fact, not only competition but also cooperation or a combination between the two types of synchronization is possible. This can especially be achieved if the problem is extended to the field of globally coupled maps [35,36] and complex network with delayed feedback and coupling [37–39].

In the following, after a brief introduction to the two basic types of synchronization in Section 2, the synchronization combination phenomenon will be discussed in Section 3. Simulation results show that when $\eta_{12} \neq \gamma$ a synchronization $I_2(t-\tau) \sim I_1(t-\tau_{c12})$ (AS) still exists. Though it is not good in quality and often hidden behind, it can play an important role in the synchronization combination. That is to say, combination between LS (introduced by a conversing coupling with a suitable delay) and the originally hidden anticipatory synchronization may produce a relatively good synchronization. A discussion concludes the paper.

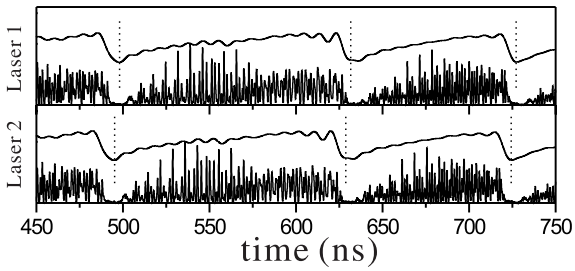

Fig. 2. Time traces of two unidirectional coupled lasers operating in an LFF regime, typically showing anticipatory synchronization with parameters: $\gamma = 8\ \mathrm{ns}^{-1}$, $\eta_{12} = 8\ \mathrm{ns}^{-1}$, $\tau = 7$ ns, $\tau_{c12} = 4$ ns, $j = 1.003$, $\alpha = 5$, $k = 500\ \mathrm{ns}^{-1}$, $\tau_n = 1$ ns. Vertically shifted low-pass-filtered ones are plotted in solid lines to emulate the experimental detection, clearly exhibiting the dropout events [17].

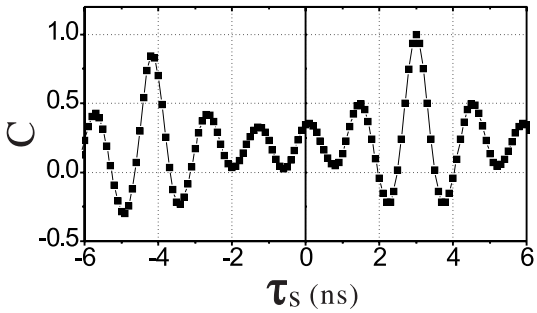

Fig. 3. Plot of the correlation function C as a function of shift time τ_s, corresponding to the typical anticipatory synchronization in Figure 2.

2 Anticipatory and lagged synchronization

In this section, the two basic types of synchronization will be reviewed. Numerical simulation is performed by Lang-Kobayashi (LK) equations for the complex electric fields E and normalized carrier densities N [40]

$$\frac{dE_1}{dt} = k(1+i\alpha)[G_1 - 1]E_1(t) + \gamma_1 E_1(t-\tau)e^{(-i\omega_1\tau)}, \quad (3)$$

$$\frac{dN_1}{dt} = \frac{j - N_1 - G_1|E_1|^2}{\tau_n}, \quad (4)$$

$$\frac{dE_2}{dt} = k(1+i\alpha)[G_2 - 1]E_2(t) + \eta_{12} \times E_1(t-\tau_{c12})e^{[-i(\omega_1\tau_{c12}+\triangle\omega t)]}, \quad (5)$$

$$\frac{dN_2}{dt} = \frac{j - N_2 - G_2|E_2|^2}{\tau_n}. \quad (6)$$

The subscripts 1 and 2 denote *laser 1* and *laser 2* respectively. The second term in equation (3) corresponds to the feedback in *laser 1*, and the second term in equation (5) corresponds to the coupling from laser 1 to laser 2, k represents the cavity loss, α is the linewidth enhancement factor, $G = N/(1+\epsilon|E|^2)$ represents the optical gain, ϵ stands for the gain saturation coefficient, ω for the optical frequency without feedback, $\triangle\omega = \omega_2 - \omega_1$ for the frequency detuning, j stands for the normalized injection current, and τ_n for the carrier lifetime.

Two types of synchronization are shown in the following two cases respectively.

In the first case, a typical anticipatory synchronization is shown with the following parameters: $\eta_{12} = \gamma = 8\ \mathrm{ns}^{-1}$, $\tau = 7$ ns, $\tau_{c12} = 4$ ns. The intensity outputs of the two lasers are plotted in Figure 2. The two lasers are both operating in an LFF regime, where a sudden output reduction (a dropout) appears, followed by a gradual recovery, until another dropout occurs. The intervals between dropouts are irregular. In order to remove the fluctuations in high frequencies to underline the dropout events, the low-pass-filtered diagrams are plotted and shifted upward. The dropout events are labeled by short dotted lines.

As clearly shown in Figure 2, the two lasers undergo dropouts in the same place due to the synchronization achieved. In addition, 3 ns before every dropout in laser 1 there is always a corresponding dropout in laser 2. This is a typical AS, satisfying equation (1).

Figure 3 shows a correlation function C between the outputs of the two lasers shown in Figure 2 as a function of the shift time τ_s. The correlation function C is defined as follows:

$$C(\tau_s) = \frac{\langle [I_1(t+\tau_s) - \langle I_1\rangle][I_2(t) - \langle I_2\rangle]\rangle}{\{\langle [I_1(t) - \langle I_1\rangle]^2\rangle\langle [I_2(t) - \langle I_2\rangle]^2\rangle\}^{1/2}}. \quad (7)$$

From Figure 3, it is seen that there is a peak at $\tau_s = 3$ ns. This peak indicates that a strong correlation can be obtained when the output of laser 2 is shifted backward by 3 ns. Obviously this peak corresponds to the AS shown in Figure 2.

Besides the right peak, there is another peak at $\tau_s \approx -4$ ns. It is noted that $\tau_{c12} = 4$ ns in the numerical simulation. This peak indicates that shifting the output of laser 2 forward by τ_{c12} can also produce a strong correlation. This left peak satisfies equation (2) and corresponds to lagged synchronization. This LS behavior is not visible in Figure 2, in spite of the fact that its correlation function (left peak) varies up to a considerable value of about $C \approx 0.9$. The two major peaks shown in Figure 3 represent two different mechanisms of AS and LS.

There is strong competition between the two mechanisms. If there is a dropout in laser 1 at a time t, there can occur a dropout in laser 2 either at time $(t - 3$ ns) or at time $(t + 4$ ns). However, the two possible dropouts cannot be both triggered. In the carrier-frequency phase space, several pairs of fixed points, usually denoted as external cavity modes and antimodes lie on an ellipse. When the system performs LFFs, the laser is observed to jump from one external cavity mode to another and try to move towards the maximum gain mode near the top of the ellipse. Before reaching it, the path goes so near an unstable antimode that it is repulsed suddenly towards the center of the ellipse, therefore a dropout is produced [16]. The jumping process among external cavity modes is necessary for LFFs and contributes the main part of the time interval between two successive dropouts, which has been shown numerically and experimentally on a time scale of 100 ns [41]. Obviously 7 ns is not long enough for the system to complete the process of jumping among external cavity modes and going near an antimode to trigger another dropout. Therefore, there is only one choice for laser 2 since the time interval is very short. On the other hand, it is not always the earliest possible dropout to be triggered. Instead, the dropout corresponding to the synchronization behavior of better quality is triggered. In the other words, the better synchronization behavior with a higher correlation is visible between the outputs of the two lasers, while the lesser one with a lower correlation is hidden. Since the right peak in Figure 3 is higher (indicating that the anticipatory synchronization is better), AS overrules LS, so LS behavior is hidden. Although only AS is visible in Figure 2, two-peaks configuration in one correlation plot implies the existence of both AS and LS.

In the second case, a typical LS is shown with the following parameters: $\eta_{12} = 8$ ns^{-1}, $\gamma = 5$ ns^{-1}, $\tau = 7$ ns, $\tau_{c12} = 4$ ns, i.e., γ is slightly decreased. The outputs of the two lasers and vertically-shifted low-pass-filtered diagrams are plotted in Figure 4, ranging from 200 ns to 450 ns. Every dropout in laser 1 is about 4 ns ahead of the corresponding dropout since $\tau_{c12} = 4$ ns. Therefore a typical LS between the two lasers can be seen here, satisfying equation (2). This synchronization is induced by the fact that the unidirectional coupling is sufficient for the laser 1 to drive the dynamics of the laser 2 which leads to a locking-state phenomenon.

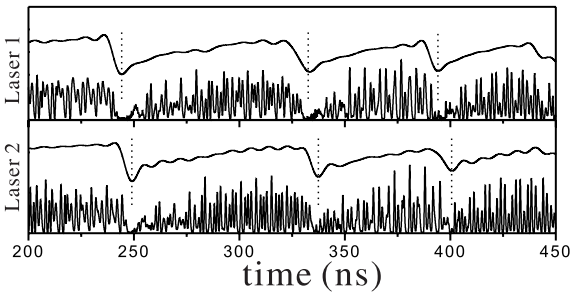

Fig. 4. Time traces of two unidirectional coupled lasers typically showing lagged synchronization with parameters: $\gamma = 5$ ns^{-1}, $\eta_{12} = 8$ ns^{-1}, $\tau = 7$ ns, $\tau_{c12} = 4$ ns. Other parameters are the same as that in Figure 2.

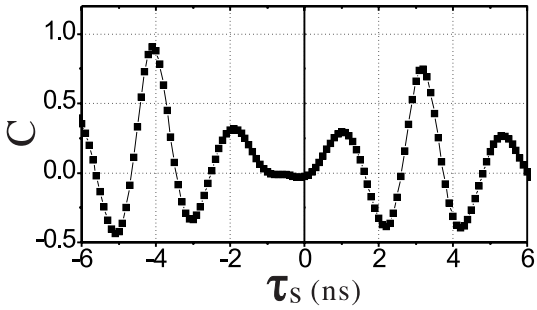

Fig. 5. Plot of the correlation function C as a function of shift time τ_s, corresponding to the typical lagged synchronization in Figure 4.

Figure 5 shows the plot of the correlation function C. The two peaks can be easily identified. The left peak corresponds to LS while the right one corresponds to AS. The right peak shows that AS still exists but lacks in quality. Though the right peak of C is about 0.75, anticipatory synchronization behavior is not visible in Figure 4 due to the fact that only the dropout corresponding to the higher correlation peak (left peak in this case) is triggered within a very short period of time 7 ns. Only because the left peak is higher than the right one (indicating that the lagged synchronization quality is better), AS is overruled by LS here and has therefore been hidden. Hence only LS is visible in Figure 4.

According to the above discussion about which type of synchronization is visible (AS or LS), the result is determined by their competition in quality. Because the dropouts corresponding to the higher correlation peak are triggered, the synchronization behavior of better quality is visible, while the lesser, although still existing within the system and being reflected by a lower correlation peak, is hidden behind and invisible.

3 Synchronization combination

AS and LS not only compete but also cooperate with each other, hence their combination. In this section, the conditions of such a combination are discussed. The prototype

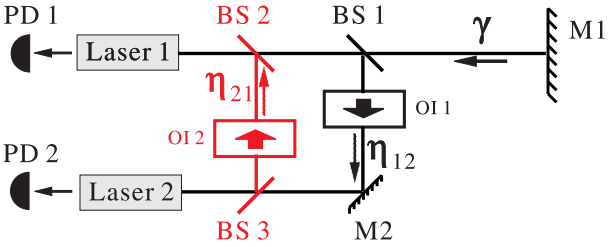

Fig. 6. Schematic representation of a bidirectional coupled laser system investigating the combination of anticipatory and lagged synchronization. The coupling from laser 1 to laser 2 travels via BS1, OI1 and M2, while the converse coupling travels from laser 2 to laser 1 via BS3, OI2 and BS2.

of the following discussion is almost the same as the second case in the previous section, except for the fact that a converse coupling with coupling strength η_{21} is used as shown in Figure 6 using the following parameters: $\eta_{21} = \eta_{12} = 8$ ns^{-1}, $\gamma = 5$ ns^{-1}. Two optical isolators are used to ensure that both couplings are unidirectional, therefore $\tau_{c21} \neq \tau_{c12}$, where τ_{c21} represents the time taken for the light to travel from laser 2 back to laser 1.

Here the right correlation peak appears due to a combination of the two factors:

(1) before adding the converse coupling, there has been an AS (hidden behind): $I_2(t-\tau) \sim I_1(t-\tau_{c12})$, where laser 1 lags behind laser 2 by the time $\tau_s = \tau - \tau_{c12}$;
(2) after adding the converse coupling, there is also an LS due to the converse coupling from laser 2 to laser 1: $I_1(t) \sim I_2(t-\tau_{c21})$, where laser 1 lags behind laser 2 by the time $\tau_s = \tau_{c21}$.

The parameters can be chosen as: $\tau = 7$ ns, $\tau_{c12} = 4$ ns, and $\tau_{c21} = 3$ ns, then $\tau_{c21} = \tau - \tau_{c12}$, leading to a combination of AS with LS at $\tau_s = 3$ ns.

The dynamical behavior of bidirectional coupled laser 1 (with a external feedback) and laser 2 (solitary) is described by the following equations [Eqs. (8) and (9)] and equations (5) and (6) respectively

$$\frac{dE_1}{dt} = k(1+i\alpha)[G_1 - 1]E_1(t) + \gamma_1 E_1(t-\tau)e^{(-i\omega_1\tau)} + \eta_{21}E_2(t-\tau_{c21})e^{[-i(\omega_2\tau_{c21} - \triangle\omega t)]}, \quad (8)$$

$$\frac{dN_1}{dt} = \frac{j - N_1 - G_1|E_1|^2}{\tau_n}. \quad (9)$$

The third term in equation (8) is added for the converse coupling.

Numerical simulations are shown in Figures 7 and 8. As expected, in Figure 7, before every dropout of laser 1, there has inevitably been a dropout in laser 2. Synchronization between the two lasers is achieved and laser 2 is ahead of laser 1 by 3 ns.

The fact that laser 2 is synchronized to the later dynamical behavior of laser 1 results from the combination of two basic types of synchronization behavior, anticipatory and lagged synchronization. The effect of the combination is also exhibited by the correlation plotted in Figure 8. The

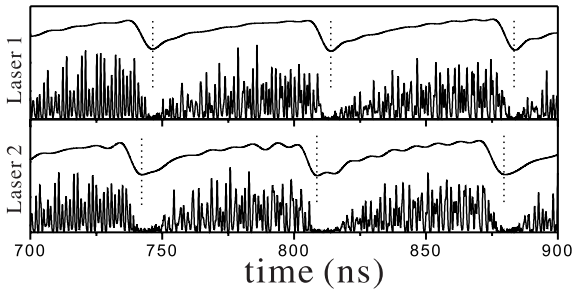

Fig. 7. Time traces of two lasers, showing the effect of the combination of anticipatory and lagged synchronization, laser 2 is seen to synchronize and lead laser 1. The parameters are chosen as $\gamma = 5$ ns^{-1}, $\eta_{12} = 8$ ns^{-1}, $\eta_{21} = 8$ ns^{-1}, $\tau = 7$ ns, $\tau_{c12} = 4$ ns, $\tau_{c21} = 3$ ns. Other parameters are the same as that in Figure 2.

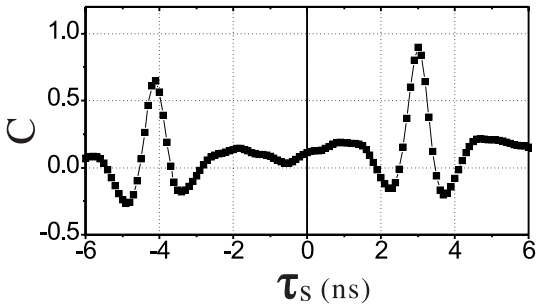

Fig. 8. Plot of correlation function C as a function of shift time τ_s, corresponding to the combination of anticipatory and lagged synchronization in Figure 7.

right correlation peak at $\tau_s = 3$ ns, reflecting the effect of the combination of AS and LS, is higher. Because the left peak at $\tau_s \approx -4$ ns, reflecting LS produced by only the coupling *from laser 1 to laser 2*, is lower, and therefore its corresponding dynamical behavior is hidden. So only the combination synchronization is visible.

If $\eta_{12} = \gamma$, AS is a complete synchronization (see Fig. 2). If η_{21} with time delay T is added to such a complete synchronization $I_2(t) = I_1(t+T)$, there is no doubt that laser 2 is always ahead of laser 1. But in Figure 7, $\eta_{12} = 8$ ns^{-1}, $\gamma = 5$ ns^{-1}, the resulting AS is not complete, it is of low quality (see Fig. 5). After introducing a converse coupling, laser 2 is ahead of the laser 1 (see Fig. 7). When no converse coupling is added, laser 1 leads laser 2 (see Fig. 4).

It seems that the addition of the converse coupling induces laser 2 to appear ahead of the laser 1. But in the calculation, the coupling strengths in the two directions are identical, i.e. $\eta_{12} = \eta_{21} = 8$ ns^{-1}. If it is true that the converse coupling alone induces the laser 2 to appear ahead of laser 1, why doesn't the coupling η_{12} cause laser 1 to go ahead of laser 2 in the same way? But that does not happen. So the converse coupling alone cannot account for the fact that laser 2 is always ahead of laser 1. In addition the LS (introduced by η_{21}, no advantage over the LS introduced by η_{12}) and the AS (lacking in quality) combine to produce a better synchronization, so that laser 2 always leads laser 1 in time, which may be a reasonable

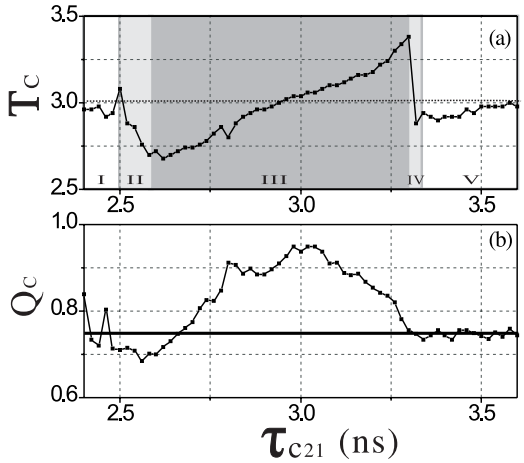

Fig. 9. Plot of the dependence of T_c and Q_c on the converse coupling retardation time τ_{c21}, ranging from 2.4 ns to 3.6 ns. All the parameters are the same as that in Figure 7.

explanation. On the other hand, the combination further proves the existence of the AS when $\eta_{12} \neq \gamma$. Indicated by the right peak in Figure 5, the AS is usually hidden behind and ignored, but it plays a crucial role in the combination concerned here.

It is interesting to note that the matching condition $\tau_{c21} = \tau - \tau_{c12}$ induces the combination of AS and LS to create a strong correlation and consequent *combination synchronization*. For further discussion about the effect of the combination of AS and LS, a more general setting is necessary where $\tau_{c21} \neq \tau - \tau_{c12}$. This is achieved by moving the branch of the converse coupling so that τ_{c21} is modified.

In the following discussion, combination synchronization quality Q_c and its characteristic time scale T_c will be investigated:

$$Q_c = \max(C(\tau_s)), \quad \tau_s > 0, \tag{10}$$

$$C(T_c) = Q_c, \tag{11}$$

where T_c is the lag time between the two lasers.

(1) In AS, laser 1 lags behind laser 2 by the time dependent on the difference of the external cavity round trip time of laser 1 and the coupling retardation time, i.e. $\tau - \tau_{c12}$, independent of the converse coupling retardation time τ_{c21}. When τ_{c21} is increased, the lag time should remain almost unchanged.

(2) In LS, laser 1 lags behind laser 2 by the time dependent on the converse coupling retardation time τ_{c21}. When τ_{c21} is increased, the lag time should be increased proportionally.

Within the combination of AS and LS, will the lag between the two lasers (T_c) change proportionally or remain equal when τ_{c21} is increased?

Figure 9 shows the dependence of T_c (a) and combination synchronization quality Q_c (b) on the converse coupling retardation time τ_{c21}. The results show the range of τ_{c21} from 2.4 ns to 3.6 ns, which can be divided into five regions, labeled I-V. In region I and V, T_c remains equal and always stays near 3.0 ns. This fact indicates that when τ_{c21} largely differs from $\tau - \tau_{c12}$ in region I and V, AS behavior is exhibited and is more prominent in the combination of AS and LS. Furthermore, it is seen in Figure 9b that the corresponding Q_c nearly equals the quality of AS shown by the height of the right peak in Figure 5, where the converse coupling is still not added, and is also lined out in Figure 9b by a straight line. It seems that when two characteristic time scales $\tau - \tau_{c12}$ and τ_{c21} differs largely, the combination effect is not so great as to enhance the synchronization quality. In region III where τ_{c21} is close to $\tau - \tau_{c12}$, T_c always approximately equals τ_{c21} ($T_c \approx \tau_{c21}$), presenting a striking contrast to region I and V. The fact that T_c increases with τ_{c21} in region III implies that LS behavior is prominent and becomes the decisive force in the combination of AS and LS. In addition, the quality of the combination synchronization mostly surpasses the straight line, indicating that the combination of LS and AS has produced a better synchronization than only AS in most parts of region III. The maximum efficiency of the combination is obtained at about $\tau_{c21} = 3$ ns ($\tau - \tau_{c12} = 3$ ns). Regions II and IV are transition regions. T_c falls rapidly from $\tau - \tau_{c12}$ to τ_{c21} in region II, and from τ_{c21} back to $\tau - \tau_{c12}$ in region IV. In these transition regions it may occur that neither AS nor LS is prominent in the combination. In this case the quality of the resulting combination synchronization is even worse than AS only, especially in region II.

4 Discussion

It is noted that in Figure 7, where the combination synchronization is demonstrated, both couplings are of the same strength, i.e. $\eta_{12} = \eta_{21}$. If the feedback in laser 1 is removed, the system will become a typical Face-to-Face (F2F) model [42,43]. In the F2F model, synchronization can be obtained with a time lag between two lasers. The leader role switches from one laser to the other randomly and continuously because of the symmetry. The investigation of synchronization combination may provide another way to understand why laser 2 always leads laser 1 after a delayed feedback is added to laser 1.

A simple analysis of the rate equations for the unidirectional laser system has identified the required matching condition $\eta_{12} = \gamma$ (no feedback in laser 2) is necessary for the existence of anticipatory synchronization. In fact, when the stringent matching condition is not satisfied, AS still exists, but lacks in quality, and is therefore always hidden. As shown in Figure 7, AS of lesser quality has even become an important factor in the synchronization combination.

Sivaprakasam et al. experimentally demonstrated a synchronization phenomenon between two bidirectional coupled lasers [44,45]. Their setup configuration is the same as that shown in Figure 6 of this paper except that $\tau_{c12} = \tau_{c21}$ in their setup. Their experiments show the "slave" can be synchronized to the future state of the "master" and the corresponding "anticipating time" always equals to the coupling retardation time. It is our opinion that the experimentally obtained synchronization

may be due to the combination of synchronization. In region III of Figure 9 of this paper, $T_c = \tau_{c21}$, a correlation with Sivaprakasam's experimental result can be found.

It is a pleasure to thank A. Campenhausen and I. Campenhausen for their careful reading of the manuscript and improvement of the English. The financial support from the Natural Science Foundation of Jiangsu Province (Grant No. BK2001138) is gratefully acknowledged.

References

1. L.M. Pecora, T.L. Carroll, Phys. Rev. Lett. **64**, 821 (1990)
2. H.G. Winful, L. Rahman, Phys. Rev. Lett. **65**, 1575 (1990)
3. R. Roy, K.S. Thornburg, Phys. Rev. Lett. **72**, 2009 (1994)
4. T. Sugawara, M. Tachikawa, T. Tsukamoto, T. Shimizu, Phys. Rev. Lett. **72**, 3502 (1994)
5. G.D. VanWiggeren, R. Roy, Science **279**, 1198 (1998)
6. J.-P. Goedgebuer, L. Larger, H. Porte, Phys. Rev. Lett. **80**, 2249 (1998)
7. S. Sivaprakasam, K.A. Shore, Opt. Lett. **24**, 466 (1999)
8. I. Fischer, Y. Liu, P. Davis, Phys. Rev. A **62**, 011801(R) (2000)
9. H. Fujino, J. Ohtsubo, Opt. Lett. **25**, 625 (2000)
10. V. Ahlers, U. Parlitz, W. Lauterborn, Phys. Rev. E **58**, 7208 (1998)
11. C.R. Mirasso, P. Colet, P. Garcia-Fernández, IEEE Photon. Electron. Lett. **8**, 299 (1996)
12. V. Annovazzi-Lodi, S. Donati, A. Scire, IEEE J. Quantum Electron. **32**, 953 (1996)
13. T. Heil, I. Fischer, W. Elsässer, Phys. Rev. A **58**, R2672 (1998)
14. C. Risch, C. Voumard, J. Appl. Phys. **48**, 2083 (1977)
15. C.H. Henry, R.F. Kazarinov, IEEE J. Quantum Electron. **22**, 294 (1986)
16. T. Sano, Phys. Rev. A **50**, 2719 (1994)
17. I. Fischer, G.H.M. van Tartwijk, A.M. Levine, W. Elsässer, E. Göbel, D. Lenstra, Phys. Rev. Lett. **76**, 220 (1996)
18. A. Hohl, H.J.C. van der Linden, R. Roy, Opt. Lett. **20**, 2396 (1995)
19. D.W. Sukow, J.R. Gardner, D.J. Gauthier, Phys. Rev. A **56**, R3370 (1997)
20. F. Marino, M. Giudici, S. Barland, S. Balle, Phys. Rev. Lett. **88**, 040601 (2002)
21. J.M. Buldú, J. García-Ojalvo, M.C. Torrent, Phys. Rev. E **69**, 046207 (2004)
22. I. Wallace, D. Yu, W. Lu, R.G. Harrison, Phys. Rev. A **63**, 013809 (2000)
23. C. Masoller, Phys. Rev. Lett. **86**, 2782 (2001)
24. Y. Liu, Y. Takiguchi, P. Davis, T. Aida, S. Saito, J.M. Liu, Appl. Phys. Lett. **80**, 4306 (2001)
25. S. Tang, J.M. Liu, Phys. Rev. Lett. **90**, 194101 (2003)
26. K. Kusumoto, J. Ohtsubo, IEEE J. Quantum Electron. **39**, 1531 (2003)
27. A. Locquet, F. Rogister, M. Sciamanna, P. Mégret, M. Blondel, Phys. Rev. E **64**, 045203(R) (2001)
28. A. Locquet, C. Masoller, P. Mégret, M. Blondel, Opt. Lett. **27**, 31 (2002)
29. A. Locquet, C. Masoller, C.R. Mirasso, Phys. Rev. E **65**, 056205 (2002)
30. E.M. Shahverdiev, K.A. Shore, Phys. Lett. A **295**, 217 (2002)
31. A. Murakami, J. Ohtsubo, Phys. Rev. A **65**, 033826 (2002)
32. I.V. Koryukin, P. Mandel, Phys. Rev. E **65**, 026201 (2002)
33. L. Wu, S. Zhu, Phys. Lett. A **315**, 101 (2003)
34. S. Sivaprakasam, P.S. Spencer, P. Rees, K.A. Shore, Opt. Lett. **27**, 1250 (2002)
35. N.F. Rulkov, Phys. Rev. Lett. **86**, 183 (2001)
36. M. Dhamala, V.K. Jirsa, M. Ding, Phys. Rev. Lett. **92**, 074104 (2004)
37. M. Barahona, L.M. Pecora, Phys. Rev. Lett. **89**, 054101 (2002)
38. F.M. Atay, J. Jost, A. Wende, Phys. Rev. Lett. **92**, 144101 (2004)
39. R. Albert, A.-L. Barabási, Rev. Mod. Phys. **74**, 47 (2002)
40. R. Lang, K. Kobayashi, IEEE J. Quantum Electron. **16**, 347 (1980)
41. J. Mulet, C.R. Mirasso, Phys. Rev. E **59**, 5400 (1999)
42. T. Heil, I. Fischer, W. Elsässer, J. Mulet, C.R. Mirasso, Phys. Rev. Lett. **86**, 795 (2001)
43. J. Mulet, C. Masoller, C.R. Mirasso, Phys. Rev. A **65**, 063815 (2002)
44. S. Sivaprakasam, E.M. Shahverdiev, P.S. Spencer, K.A. Shore, Phys. Rev. Lett. **87**, 154101 (2001)
45. P. Rees, P.S. Spencer, I. Pierce, S. Sivaprakasam, K.A. Shore, Phys. Rev. A **68**, 033818 (2003)